ECS Transactions, 58 (22) 1-14 (2014)
10.1149/05822.0001ecst ©The Electrochemical Society

# Applications of AC Impedance Spectroscopy as Characterization and Diagnostic Tool in Li-metal Battery Cells

**Vadim Lvovich*, James Wu, William Bennett, Brianne DeMattia, Thomas Miller**

*NASA Glenn Research Center,*
*Electrochemistry Branch, Power and In-Space Propulsion Division,*
*21000 Brookpark Rd., Cleveland, OH 44135*

## Abstract

Electrochemical Impedance spectroscopy (EIS) is an exceptionally powerful and rapidly evolving technique for investigating electrical properties of materials and electrochemical interfacial kinetic processes in a wide variety of practical systems and applications. The method offers the most powerful on-line and off-line analysis of the status of investigated media, electrodes, and probes in many different complex time– and space-resolved processes that occur in electrochemical laboratory experiments or over a lifetime of monitored samples, devices, or materials. EIS is useful as an empirical quality control procedure that can also be employed to interpret fundamental electrochemical processes (1, 2).

At NASA Glenn Research Center the EIS technique is being widely and effectively employed in characterization and performance monitoring of rechargeable energy storage devices, such as states of electrodes during charging / discharging cycles in secondary batteries and fuel cells. The technical objective for batteries is to improve the performance of rechargeable cells to meet the energy storage requirements of human missions. The approach is to develop advanced battery components to safely provide substantially higher specific energy for relatively few charge/discharge cycles. In the presented work, impedance spectroscopy and other electrochemical and surface science techniques have been widely applied to monitoring developed lithium-metal battery (LMB) cells, including investigation of the impact of novel ionic liquid electrolytes on cycle life and dendrite growth/suppression on Li anodes. Applications of EIS method allowed for efficient in situ performance monitoring of various types of electrodes and electrolytes used in experimental battery cells. The studies were focused initially on evaluating performance of separate battery components in symmetric lithium coin cells, with a purpose of future complete impedance analysis of full cells with Li anode and dedicated cathode.

* - corresponding author. Tel.: (216)433-5261.
*E-mail address:* vadim.f.lvovich@nasa.gov

## Introduction

Green aviation's goals of high energy efficiency, low emissions and reduced noise can be achieved with electric aircraft. A principal barrier to electric aviation is high capacity energy storage. Li-ion batteries (LIB) with metal oxide cathodes, graphite anodes, and organic liquid electrolytes represent the state-of-the-art. However, LIBs have issues in terms of safety and thermal stability. In addition, LIBs fall short of meeting the power and energy requirements for electric aircraft (3). Breakthroughs beyond the current state-of-the-art in battery technology are necessary to fully realize green aviation.

Li metal anodes combined with advanced cathode materials such as Li-Air or Li-Sulfur offer substantial weight reduction and the promise of 5X improvements in specific energies, e.g. 1000 Wh/kg (Li-Air) compared to 200 Wh/kg for LIB (4). The *fundamental* obstacle to the use of Li metal anodes in advanced, rechargeable, high energy batteries is poor charge/discharge cycling efficiency and safety concerns due to dendrite formation at the anode-electrolyte interface which can cause internal short circuits. Alternative electrolytes based on non-flammable, thermally and electrochemically stable ionic liquids (mixtures of cations and anions) have the potential to solve these problems. For example, recent work has shown certain ionic liquids (IL) electrolytes may suppress the formation of dendrites and show improved cycling capabilities relative to traditional organic electrolytes (5). The number of possible ionic liquids and other similar electrolytes is vast, and while some ILs show dendrite suppression, others do not. Identifying the fundamental factors controlling the performance of these ultra-high energy Lithium metal batteries (LMB) as well as developing tools for rapid screening and selection of optimal components for fabrication is required to assess fully their potential.

The experimental work described in this paper was performed under a joint effort between the NASA Glenn Research Center and NASA Ames Research Center. The objective of this work is to develop an integrated experimental/computational infrastructure to accelerate fundamental understanding, screening and design of novel IL electrolytes for advanced ultra-high energy LMBs. The novelty of our approach results from the combination of validated computational modeling with experimental screening to produce a reliable predictive capability for the selection of optimal components, their fabrication parameters, and the design of ultra-high energy LMB that can meet energy storage challenges of current and future NASA missions and many terrestrial transportation application such as electric vehicles and aircraft. This publication is focused on experimental results, a separate paper dedicated to computational modeling aspects of this study will be published later.

## Experimental Procedures

Two different IL electrolytes were considered: 1-butyl-1-methylpyrrolidinium bis(fluoro-sulfonyl)imide ([pyr14][TSFI]) (6) which has shown to form a stable SEI layer which promotes stable cycling with Li metal, and non-trivial dendrite suppression in laboratory systems, and Li anode cycling ability on the order of 1000 cycles in laboratory systems. Second electrolyte, 1-ethyl-3-methyl imidazolium tetrafluoroborate ([EMIM][$BF_4$]) which has shown little or no dendrite suppression and very poor cycle life with Li metal (7). The literature studies with [EMIM][$BF_4$] have demonstrated short-circuiting due to dendrite growth in as little as 100 cycles. Note that pyr14 and EMIM are cations and TSFI and $BF_4$ are anions. Chemical structures are shown in Figure.

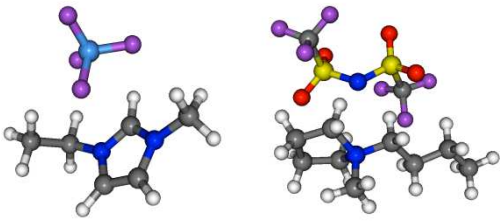

**Figure 1. Chemical structure for ionic pairs of [EMIM][BF4] (left) and [pyr14][TSFI] (right)**

For these two cases, several essential elements were considered. First, the bulk electrical properties of isolated ILs important for battery operation were determined. Second, the structure and electrochemical properties of the IL in the presence of an electrode were investigated; interaction of the ILs with the anode surface affects the local molecular ordering of the IL as well as its properties. Third, chemical reactions between the IL electrolyte and the Li metal anode surface at zero applied voltage were considered. Fourth, laboratory LMBs using the two ILs were built and characterized.

Experimental studies characterized fundamental properties of electrolytes including ionic conductivity to evaluate the performance of each electrolyte in laboratory LMBs. Electrochemical impedance spectroscopy (EIS) helped further characterize the performance of the electrolytes in LMBs. EIS scans, performed over the lifetime of a cell, identify sources of performance loss (loss of ionic conductivity, surface area development, and resistive film growth). Electrolytes' compatibilities with electrode materials were investigated via cyclic voltammetry (CV). CV helps to identify the presence of undesirable decomposition reactions, as well as the required Li plating and stripping processes which are essential for a viable LMB. After cycling, cell components were examined for evidence of morphology changes and visual evidence of decomposition of the electrolyte. Scanning electron microscopy (SEM) was used to characterize morphology changes, including dendritic growth, of the cycled electrodes. Optical microscopy was performed to visually characterize the nature of the electrode surface deposits. Energy dispersive X-ray spectroscopy (EDS) provided evidence of elemental compositions of the morphological features. This work revealed the physical changes of the Li electrodes after cycling, and identified possible decomposition products on the surface. Properties and performance were assessed and could be compared to the traditional battery metrics.

Coin cells were used as the standard test vehicle because are easy to assemble and provide reproducible data that can be used to assess the performance of the ionic liquid in cell format. This effort focused on the use of symmetric coin cells utilizing two electrodes of lithium metal. The symmetric coin cell allows the ionic liquid to be tested directly with lithium metal as both the cathode and anode, removing the level of uncertainty which may arise with the use of a standard cathode material whose reactions and interactions with these ionic liquids may be unknown. Figure 2 illustrates the construction of a symmetric lithium metal coin cell.

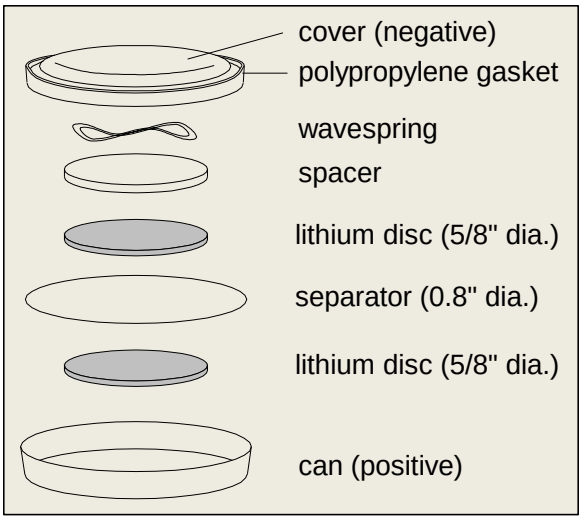


**Figure 2. Symmetric coin cell construction**

Several sets of coin cells were constructed containing the [pyr14][TFSI] and [EMIM][$BF_4$] ionic liquid electrolytes. Each cell was "flooded" with 30µL of electrolyte to ensure the coin cell contained a sufficient volume. The lithium metal electrodes used for these coin cells were 5/8-inch diameter discs of 0.005-inch to 0.03 inch thicknesses. The separator used was a Celgard M825, a 16µm tri-layer material commonly used in lithium ion cells.

Once the symmetric coin cells were constructed, cycling was performed at a controlled constant current of ±0.1mA/$cm^2$, with the area calculated based on the area of one lithium metal electrode, in a controlled 20°C environment. This current was consistent with similar work done in this area (4). Cycling allows for the observation of the ability of the electrolyte to transfer Li efficiently without undesirable reactions in the presence of Li metal. Unless otherwise noted, these were the standard materials and conditions used in most coin cell experiments.

## Experimental Results

The ultimate goal of this study was to determine why one IL promotes stable cycling with dendrite suppression while the other does not. To assess their effectiveness as electrolytes, it was important to understand their structure, thermodynamics, transport properties and electrochemical stability. Understanding the suppression mechanism will lead to the design of new electrolytes that will ultimately solve this long-standing problem and will result in dramatic improvements in battery storage capacity.

For battery applications, it is important to understand the behavior of electrochemical interfaces under an applied voltage. Under an applied voltage, charge accumulates on the electrode surface generating an electric field in the electrolyte. The electrolyte responds by forming a layer of opposite charge at the interface. This electrochemical double layer (EDL) is fundamental in electrochemistry. Hence, an experimental effort was performed to assess the electrochemical performance of each material.

An initial set of two coin cells with [pyr14][TFSI] electrolyte cycled with a 30-minute cycle regime, or 15-minute charges with 15-minute discharges and no rest periods. These cells cycled for over 3000 cycles within a symmetric 30-minute voltage window as shown in Figure 3 indicating a stable and repetitive cycling where the cells remained healthy without apparent dendrite growth and resulting causing short-circuiting.

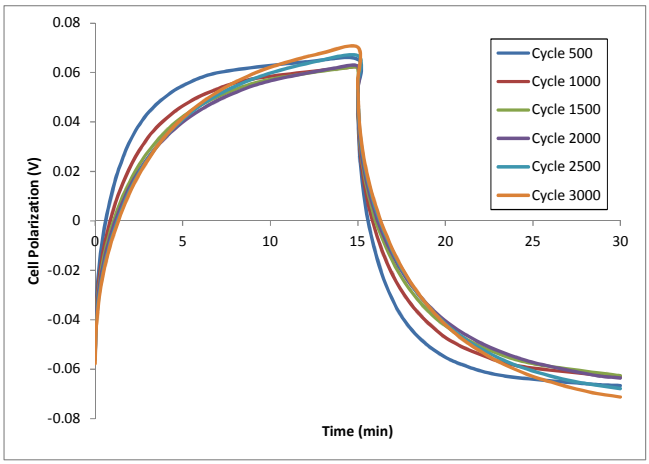


**Figure 3. [pyr14][TFSI] coin cell symmetric cycling with 0.030" Li metal**

Figure 4 shows very symmetric cycling of a [pyr14][TFSI] Li metal cell for over 1750 cycles, indicating the cell remained healthy and had not been short-circuited due to dendrite growth. It is assumed the difference in cycles accrued between this experiment and the original is due to the shift to using 0.015" thickness lithium metal.

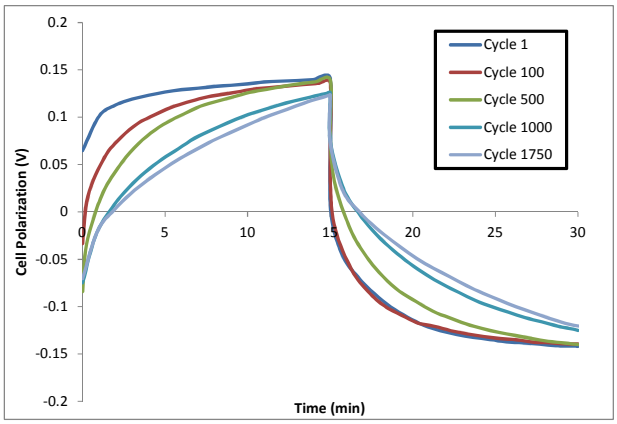


**Figure 4. [pyr14][TFSI] coin cell symmetric cycling with 0.015" thickness Li metal**

Of interest in these experiments was the effect of rest periods between half-cycles. To observe this effect, 5-minute rests were added between charge/discharge periods in the 30-minute cycle regime, essentially increasing the total cycle time to 40 minutes. These cells cycled within a tighter voltage window, but the same trend of decreasing polarization with increasing cycles was observed (Figure 5).

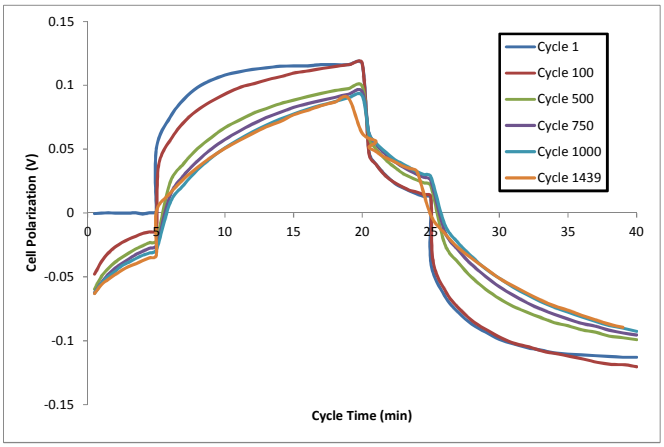


**Figure 5. [pyr14] symmetric cycling with rests**

Also of interest was the effect of longer cycle times on the lifetime and cycling characteristics of the cells. These cells were tested with a 2-hour cycle regime, or 60-minute charge/discharge periods, which represents a more realistic cycle period for real-world battery use. As Figure 6 depicts, these cells showed similar trends with symmetric cycling, but the polarization slightly increased between cycles 100 and 500.

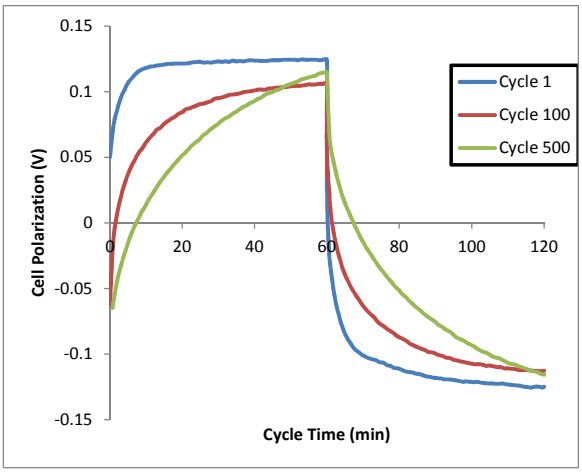


**Figure 6. [pyr14][TFSI] coin cells with 2-hour cycles**

Significantly more effort went into the cycling of [EMIM][BF4] ionic liquid because initial experiments produced coin cells with [EMIM][BF4] that would not cycle. It was determined through wetting experiments that [EMIM][BF4] was not successfully wetting the Celgard M825 separator. Without electrolyte filling the pores of the separator, the cell will not conduct ions and cannot cycle. In order to cycle [EMIM][BF4], different separators were investigated.

Since the selected separator did not cycle, two alternative separators were investigated – Hollingsworth & Vose (H&V) and glass fiber. Initial experimentation with both alternative separators showed little to no wetting at 20°C. By applying five drops of electrolyte to the separator and putting under vacuum for 8 hours at 60°C, the wettability improved. Once it was visually confirmed that the separator was wetted and additional drops of electrolyte were added to ensure the cell was "flooded", the coin cells were constructed and cycled for 20-minute cycles. Initially these coin cells showed low cell functionality and high cell impedance at 20°C. By increasing the test temperature to 60°C, the cells were able to cycle and a significant decrease in impedance was observed. The glass fiber separator coin cell cycled for only 20 cycles at 60°C before the cell polarized in one direction, so this separator was abandoned and focus shifted to the H&V separator. The cell with H&V separator cycled for over 100 cycles at 60°C, but the cells continued to polarize as cycles accrued, which is the opposite trend witnessed with [pyr14][TFSI]. Figure 7 depicts this increase in polarization as the cell cycled.

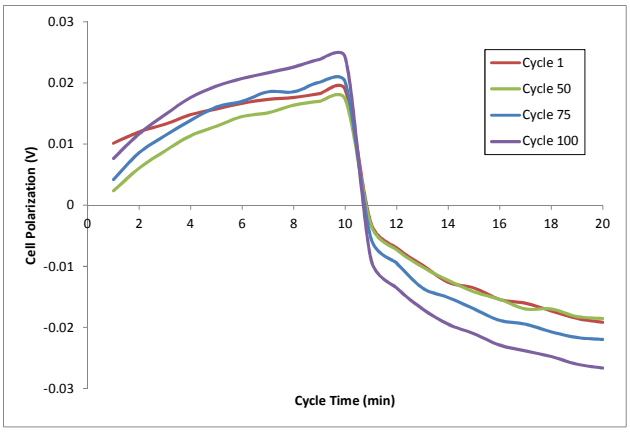


**Figure 7. [EMIM][BF4] coin cells with H&V Separator**

Most successful cells containing "electrochemical grade" [EMIM][BF4] cycled for roughly 150 cycles, slightly higher than the lower purity material, before polarizing in the negative voltage direction, possibly due to lithium plating on one electrode and failing to strip back upon discharge (Figure 8). Overall, the "electrochemical grade" ionic liquid did not have a significant impact on the performance in coin cells.

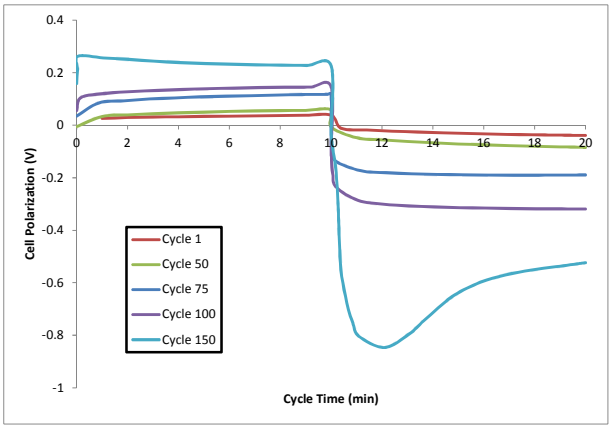


**Figure 8. [EMIM][BF4] Electrochemical grade coin cell with H&V separator**

Via electrochemical impedance spectroscopy, the internal impedance of the coin cells was measured at different intervals, including beginning of life, to quantify changes in resistance over time. The complex impedance (Nyquist) plot reveals two overlapping semicircular features in the high and medium frequency regimes, followed by a well-resolved apparently semicircular feature at the low frequencies (Figure 9), with the x and y axes in units of Ohms. It would be logical to assign the high and medium frequency features to the surface film and predominant charge transfer processes, and the low frequency impedance feature to the finite transmission-boundary diffusion, expected in the systems with small separation between the working and the counter electrodes. The surface film + charge transfer impedance of a [pyr14][TFSI] / Li metal cell decreased with cycling (Figure 9), consistent with increasing surface area of the Li metal electrodes as will be observed via microscopic analysis.

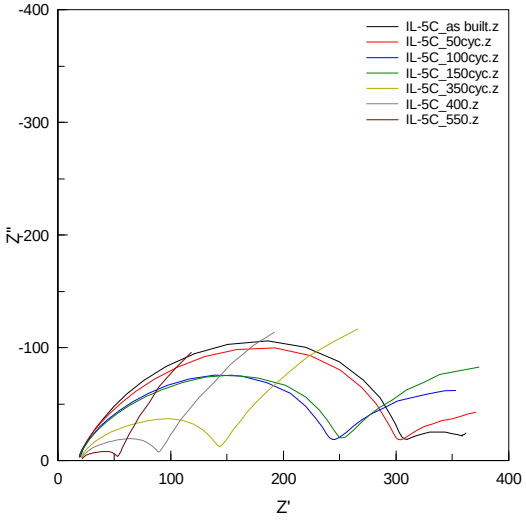


**Figure 9. Impedance spectra for [pyr14][TFSI] cells**

To the contrary, in the cells containing [EMIM][BF4] electrolyte the surface film + charge transfer impedance data trend shows increasing resistance with cycling (supporting the cycling data), which is consistent with the growth of a resistive film or decomposition of the electrolyte. Figure 10 depicts the large resistance of the cell at 20°C with an inset showing the smaller, yet increasing, resistance at 60°C. On this figure, the black and red lines represent data collected at 20°C while the blue, light and dark green were collected at 60°C and are so small in comparison with 20°C that they cannot be seen on the 20°C scale. Figure 11 compares the increase in internal resistance as cells with [EMIM][BF4] are cycled with the decrease in internal resistance as cells with [pyr14][TFSI] are cycled.

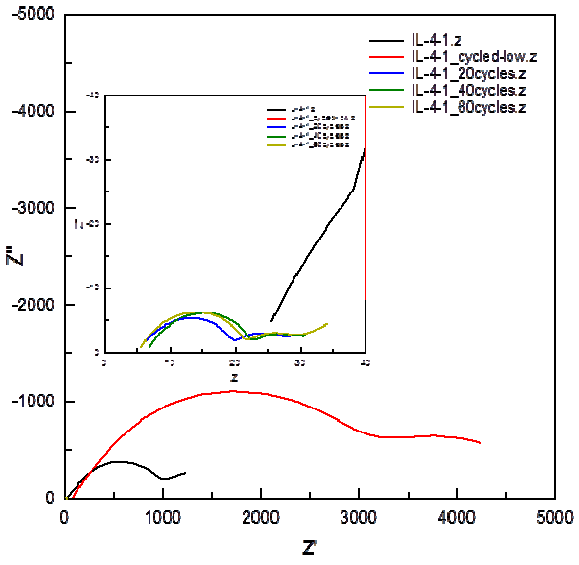


**Figure 10. Impedance spectra for [EMIM][BF4] with H&V Separator**

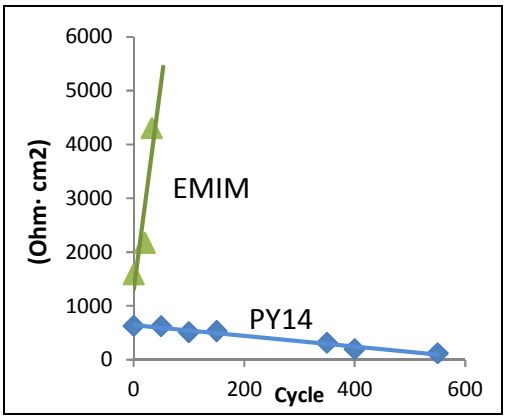


**Figure 11. Charge transfer resistance changes with cycling**

It was hypothesized that the wetting issues and poor functionality may be due to impurities in the [EMIM][BF4], so a purer "electrochemical grade" was obtained and tested (>99% versus >98%). Wetting experiments were repeated with H&V and both Celgard separators. Again, the separators were soaked at 60°C overnight and all were visibly wet before constructing the cells. Performance with either Celgard separator remained poor as neither cycled at 20°C and produced only limited cycles at 60°C.

Voltage polarization and increasing internal resistance are consistent with growth of a resistive film. These trends were corroborated by visual inspection SEM observations. These revealed a change in the color and consistency of [EMIM][BF4] after it had been cycled with Li metal. [EMIM] [BF4] became partially solidified with a concentrated amber color deposited onto the Li metal surface. The increase in impedance of [EMIM] [BF4] could also be due to decomposition of the electrolyte as the cell was cycled, which would also explain the limited number of cycles [EMIM][BF4] achieved. Such decomposition of [EMIM][BF4] is also consistent with the results of cyclic voltammetry experiments.

Cyclic voltammetry (CV) experiments on nickel electrodes produced clues to explain the differences in cycling with Li metal. Data for [EMIM][BF4] showed significant decomposition reactions as the electrode was driven to the potential seen at a Li electrode, with little capability for cycling (plating and stripping of Li metal). Addition of 6% VC additive improved cycling of [EMIM][BF4], and we intend to continue using this additive to study its effect on improved cycling capabilities of selected high performance electrolytes. Potential stability of [pyr14][TSFI] is significantly better than [EMIM][BF4]. In this testing, [pyr14][TSFI]- showed evidence of Li plating and stripping around 0.0 V vs. Li, with suppression of decomposition in repeated cycling: elements essential for cycling with Li metal. These differences were expected and formed the basis for selecting these materials for study. Cyclic voltammograms for these electrolytes are contrasted in Figure 12.

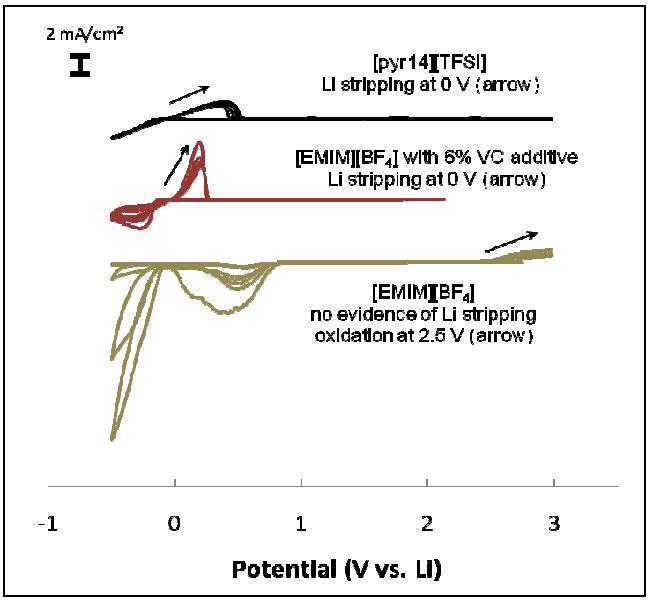


**Figure 12. Cyclic voltammetry shows Li plating and stripping for [pyr14][TSFI]. [EMIM][BF4] requires VC additive to suppress decomposition.**

Cycling efficiency information was extracted from the voltammetry data in Figure 12, by integrating current with respect to time, over five successive cycles. This analysis shows that electrolyte based on [pyr14][TSFI] develops a lithium cycling efficiency of 79% in the second cycle. In contrast, the only charge accumulation processes for [EMIM][$BF_4$]-based electrolytes correspond to electrolyte decomposition, with a cycling efficiency of essentially 0%. Capacity versus time for these electrolytes is contrasted in Figure 13. Addition of 6% VC to [EMIM][$BF_4$]-based electrolyte, dramatically improved lithium cycling capability, achieving an efficiency of approximately 50% (Figure 14).

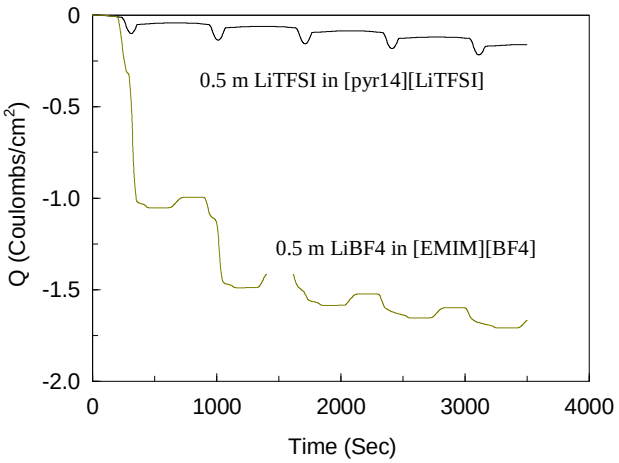


**Figure 13. Cycling efficiency of [pyr14][TSFI]-based electrolyte and [EMIM][BF4]-based electrolytes.**

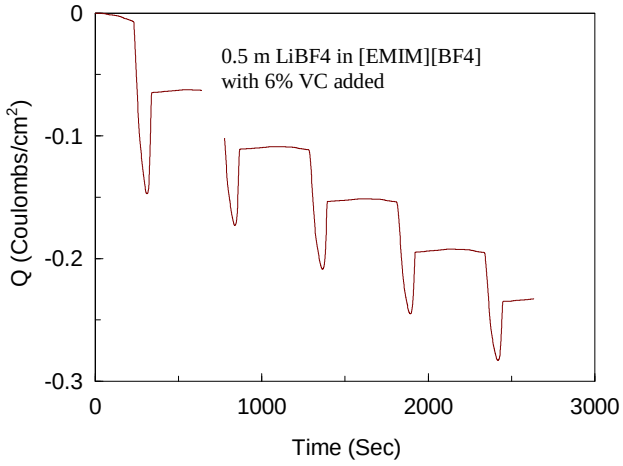


**Figure 14. Enhancement of cycling efficiency of [EMIM][BF4]-based electrolyte with 6% VC additive.**

Our computational modeling, which is a subject of a separate publication, showed that [pyr14][TSFI] reacts with Li and forms a protective layer, while the [EMIM][$BF_4$] does not. Li electrodes were harvested from cycled cells and examined by SEM and EDS, to observe physical changes of the Li electrodes after cycling, and identify possible decomposition products on the surface. Optical microscopy was also performed to visually characterize the nature of the electrode surface deposits.

Analysis of the Li cycled 2000 cycles, with [pyr14][TSFI]-based electrolyte, reveals a compacted mossy layer of Li, which is not strongly bound to the metallic Li underneath (Figure 15). EDS analysis revealed elements associated with the electrolyte (O, C, S, and F) concentrated in regions where the mossy layer was present. This observation is consistent with the formation of an SEI layer on the large surface area of the mossy Li. Regions where the mossy layer was removed revealed a textured Li surface. The high surface area of the mossy layer explains the reduced impedance with cycling in [pyr14][TSFI]-based electrolyte. Results showed the formation of thick waxy films on the surface of Li metal, when cycled with [EMIM][$BF_4$]-based electrolytes (Figure 16). Elemental mapping shows heavy concentrations of carbon and fluorine in the region of the films, supporting that the films have been formed by electrolyte decomposition. Cycling was limited to ~130 cycles with this electrolyte, and little evidence of dendrite growth is observed.

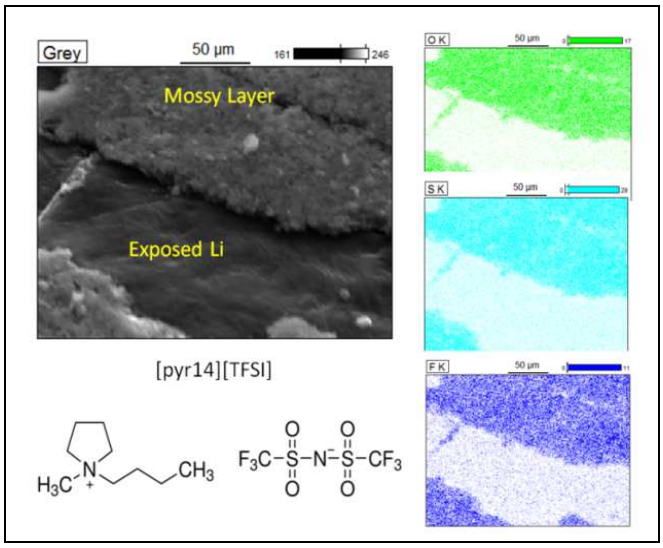


**Figure 15. SEM image of Li surface after exposure to [pyr14][TSFI] ionic liquid. Analysis shows O, S and F concentrated in mossy layers.**

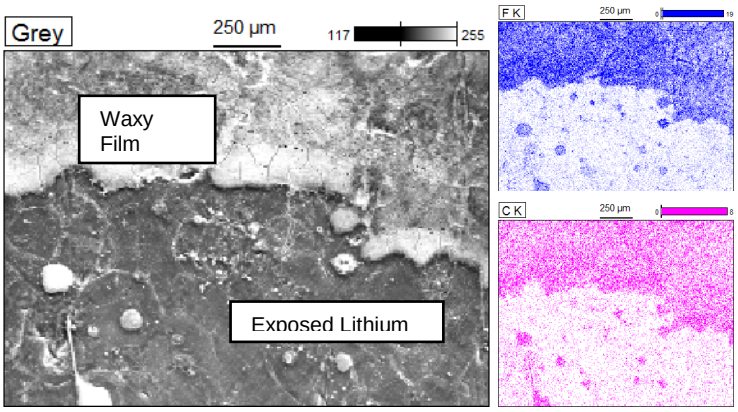


**Figure 16. SEM image of Li surface after exposure to [EMIM][BF4] ionic liquid. Analysis shows C and F concentrated in mossy layers.**

## Conclusions

This work summarizes results of electrochemical characterization of Li-metal symmetrical cells filled with two selected ionic liquid electrolytes. Overall scope of the work is directed towards performing an integrated computational-experimental investigation of the impact of novel ionic liquid electrolytes on performance characteristics, such as cycle life and dendrite growth/suppression, on Li metal electrodes in LMB. Computations will help explain experimental results obtained in this experimental work and will also be a valuable tool to support electrolyte optimization. Recently, reactive MD methods have become possible permitting simulations of reactions of much larger systems than *ab initio* but without a significant loss of accuracy.

## Acknowledgments

The author would like to acknowledge NASA Aeronautics Research Mission Directorate for financial support.

## References

1. V. Lvovich, "Electrochemical Impedance Spectroscopy - Theory and Applications, John Wiley & Sons, New York, 2012.
2. M. Orazem, B. Tribollet, “Electrochemical Impedance Spectroscopy”, John Wiley & Sons, New York, 2008.
3. NASA/CR–2011-216847, Subsonic Ultra Green Aircraft Research: Phase I Final Report.
4. M. Galiński, A. Lewandowski, I. Stępniak, „Ionic liquids as electrolytes“, *Electrochimica Acta* 51 (2006) 5567-5580.
5. N. Schweikert, A. Hofmann, M. Schulz, M. Scheuermann, S. T. Boles, T. Hanemann, H. Hahn, S. Indris, „Suppressed lithium dendrite growth in lithium batteries using ionic liquid electrolytes: Investigation by electrochemical impedance spectroscopy, scanning electron microscopy, and in situ 7Li nuclear magnetic resonance spectroscopy“, *J. Power Sources* 228 (2013) 237-243.
6. R. Bhattacharyya, B. Key, H. Chen, A. S. Best, A. F. Hollenkamp, C. P. Grey, „In situ NMR observation of the formation of metallic lithium microstructures in lithium batteries“, *Nature Mat*. 9, (2010) 504-512.
7. O. Borodin, G. D. Smith, W. Henderson, „Li+ Cation Environment, Transport, and Mechanical Properties of the LiTFSI Doped N-Methyl-N-alkylpyrrolidinium+TFSI- Ionic Liquids“, *J. Phys. Chem..B* 110, (2006) 16879-16886.